Disease-Causing Mutations in Cardiac Troponin T: Identification of a Critical Tropomyosin-Binding Region

Thomas Palm, Sarah Graboski, Sarah E. Hitchcock-DeGregori, and Norma J. Greenfield
Department of Neuroscience and Cell Biology, University of Medicine and Dentistry of New Jersey—Robert Wood Johnson Medical School, Piscataway, New Jersey 08854 USA

ABSTRACT Fifteen percent of the mutations causing familial hypertrophic cardiomyopathy are in the troponin T gene. Most mutations are clustered between residues 79 and 179, a region known to bind to tropomyosin at the C-terminus near the complex between the N- and C-termini. Nine mutations were introduced into a troponin T fragment, Gly-hcTnT$_{70-170}$, that is soluble, α-helical, binds to tropomyosin, promotes the binding of tropomyosin to actin, and stabilizes an overlap complex of N-terminal and C-terminal tropomyosin peptides. Mutations between residues 92 and 110 (Arg92Leu, Arg92Gln, Arg92Trp, Arg94Leu, Ala104Val, and Phe110Ile) impair tropomyosin-dependent functions of troponin T. Except for Ala104Val, these mutants bound less strongly to a tropomyosin affinity column and were less able to stabilize the TM overlap complex, effects that were correlated with increased stability of the troponin T, measured using circular dichroism. All were less effective in promoting the binding of tropomyosin to actin. Mutations within residues 92–110 may cause disease because of altered interaction with tropomyosin at the overlap region, critical for cooperative actin binding and regulatory function. A model for a five-chained coiled-coil for troponin T in the tropomyosin overlap complex is presented. Mutations outside the region (Ile79Asn, Δ160Glu, and Glu163Lys) functioned normally and must cause disease by another mechanism.

INTRODUCTION

Mutations in genes encoding sarcomeric proteins cause familial hypertrophic cardiomyopathy (FHC), an autosomal dominant trait characterized by ventricular hypertrophy and myocyte disarray which is often associated with sudden, premature cardiac death. The gene encoding cardiac troponin T (TnT) is one of the more frequently affected ones, accounting for ~15% of documented FHC-causing mutations (Thierfelder et al., 1994; Hernandez et al., 2001). The hcTnT mutations are mostly characterized by a very mild and many times undetectable hypertrophy. However, the rate of sudden cardiac death is often severe (Watkins et al., 1995).

Troponin T is a regulatory protein found in striated muscles that forms a complex with troponin I (TnI) and troponin C (TnC) that, together with tropomyosin (TM), is required for Ca^{2+}-dependent regulation of muscle contraction (reviewed in Perry, 1998; Gordon et al., 2000). Troponin T binds to both TnI and TnC in the Tn complex as well as to TM, and possibly actin, on the thin filament (reviewed in Perry, 1998; Gordon et al., 2000). The elongated shape of the Tn complex (Flicker et al., 1982) and its position spanning the C-terminal third or more of TM (White et al., 1987; Cabral-Lilly et al., 1997) is because of TnT (Fig. 1). The elongated N-terminal end of TnT is oriented toward the C-terminus of TM, including the head-to-tail overlap region (Pato et al., 1981; Brisson et al., 1986). The C-terminal half of TnT binds to TnI, to TnC and to the middle of TM in a Ca^{2+}-sensitive manner (Pearlstone and Smillie, 1983; Brisson et al., 1986; Pan et al., 1991).

Studies of TnT fragments have identified the critical region of the N-terminal domain. Fragments corresponding to residues ~80–180 for cardiac, and residues ~50–150 for skeletal muscle TnT, are highly α-helical, bind to TM, and increase the affinity of TM for actin (Jackson et al., 1975; Pearlstone and Smillie, 1977; Hill et al., 1992; Hinkle et al., 1999). Nine of the twelve loci of FHC-causing mutations are located in this region, the remaining three being close to the C-terminus (Fig. 1).

Despite the intensive research on FHC-causing mutations of TnT, the disease mechanism(s) is (are) poorly understood. Model systems have been developed to study the disease ranging from analysis of purified proteins to study of cardiac function in transgenic animals (reviewed in Hernandez et al., 2001). The model systems used to study the disease are complex, and sometimes the same mutation causes opposite effects in different models. For example, R92Q-TnT exchanged into skinned rabbit cardiac muscle fibers required lower levels of free Ca^{2+} for tension generation (Morimoto et al., 1998), whereas adenovirus carrying the same TnT mutant transfected into cultured rat or quail cardiac myocytes required a higher calcium concentration for tension generation (Sweeney et al., 1998; Rust et al., 1999). Similar discrepancies have been reported for other TnT mutations (Mukherjea et al., 1999; Tobacman et al., 1999; Redwood et al., 2000). Clearly, in a structure as complex as the myofibril there will be multiple disease mechanisms, and the deficiencies of a single mutation will be manifested at more than one level of contractile protein function.

Because of the difficulties of working with complex biological systems, we designed a model system to study the

Received for publication 12 April 2001 and in final form 27 July 2001.

Address reprint requests to Dr. Norma J. Greenfield, UMDNJ, Department of Neuroscience and Cell Biology, 675 Hoes Lane, Piscataway, NJ 08854-5635; Tel.: 732-235-5791; Fax: 732-235-4029; E-mail: greenfie@umdnj.edu.

0006-3495/01/11/2827/11 $2.00

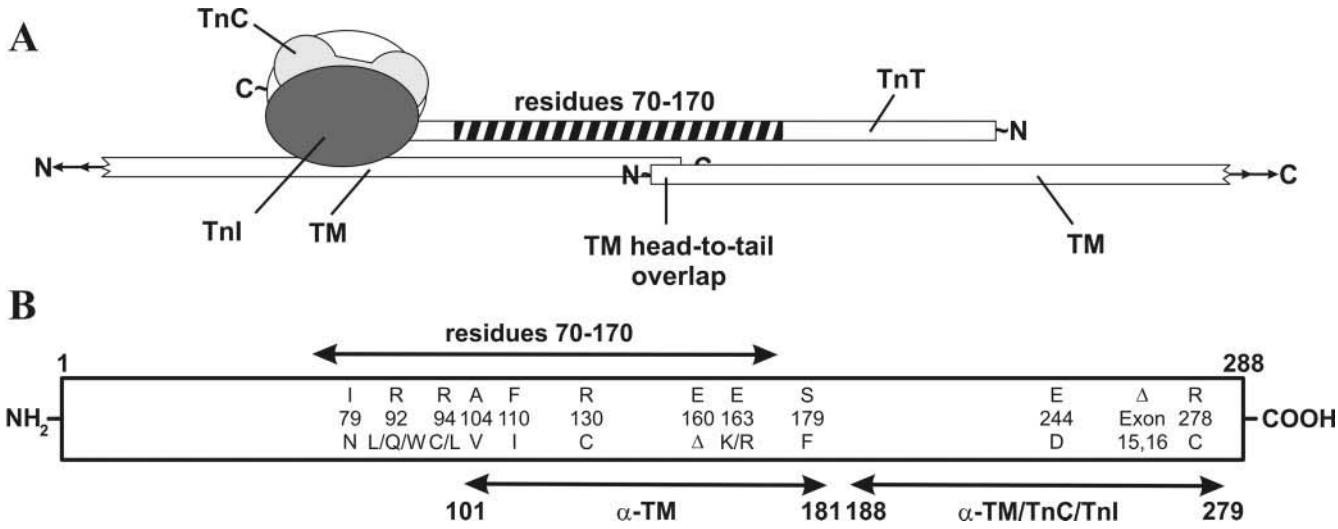

FIGURE 1 (*A*) Model of the troponin-tropomyosin complex (modified from Heeley et al., 1987). Only the first and the last ~180 residues of tropomyosin are shown. (*B*) Schematic representation of human cardiac TnT structure with sites of FHC causing mutations (modified from Bonne et al., 1998). Arrows indicate the different binding domains. References for FHC mutations are I79N, R92Q, and Δ Exon15,16 (Thierfelder et al., 1994); R92L (Forissier et al., 1996); R92W (Moolman et al., 1997); R94C (D'Cruz et al., 2000); R94L (Varnava et al., 1999); A104V (Nakajima-Taniguchi et al., 1997); F110I, ΔE160, E163K, E244D, and R278C (Watkins et al., 1995); R130C and E163R (Koga et al., 1996); and S179F (Ho et al., 2000).

effect of individual mutations on TnT function as well as its structure and stability. A fragment with residues 70–170 of human cardiac TnT, expressed in *Escherichia coli*, is soluble, binds to TM, promotes the binding of TM to actin, and stabilizes a complex with N- and C-terminal TM model peptides. Nine disease-causing mutations in this region were individually introduced into the fragment. Mutations in the residue 92–110 region altered the TM-dependent functions of this TnT fragment whereas those outside the region were neutral. We propose a model for the binding of TnT to the C-terminus of TM at the N- to C-terminal overlap region to explain the importance of the mutated residues for TnT function.

MATERIALS AND METHODS

DNA constructs

The cDNA for Gly-hcTnT$_{70-170}$ was prepared from pSBET (Schenk et al., 1995) carrying an insert encoding full-length wild-type (wt) human cardiac (hc) TnT (Thierfelder et al., 1994; Mukherjea et al., 1999). Using Pfu Turbo DNA polymerase (Stratagene, La Jolla, CA) and the polymerase chain reaction (PCR) protocol provided by the supplier, with oligonucleotides A and B (see Table 1) we inserted an N-terminal His$_6$ purification tag into full-length wt-hcTnT to create His$_6$-hcTnT in pSBET. The oligonucleotides also introduced a recognition site for tobacco etch virus (TEV) protease to allow removal of the His$_6$-tag after affinity purification, leaving an N-terminal glycine with the recombinant protein (Gly-hcTnT). The second mutagenesis step used the oligonucleotides C and D (Table 1) to insert a stop-codon following codon 170 and a *Bam*HI restriction site for cloning, creating His$_6$-hcTnT$_{1-170}$. In this step circular pSBET with full-length His$_6$-hcTnT was used as a template. Oligonucleotides B and D were 5′-phosphorylated to allow blunt end ligation of the purified PCR products. To remove the codons for the amino acids 1–69 from the cDNA, a recombinant PCR protocol was used (Higuchi, 1990). In two primary PCRs the oligonucleotide sets E, F and G, H (Table 1) were used to amplify fragments between the codon for Phe-70 and the T7-terminator, and between the T7-promotor and the last codon (Gly) of the His$_6$-tag, respectively, to create His$_6$-hcTnT$_{70-170}$. As a template for the primary PCRs we linearized His$_6$-hcTnT$_{1-170}$ in pSBET with *Bgl*II and *Eco*RI. In a secondary PCR, the overlapping primary PCR products annealed, and recessed 3′ ends were extended. Using only the outside primers from the above mentioned oligonucleotide sets, His$_6$- hcTnT$_{70-170}$ was amplified between the T7-promotor and T7-terminator. The PCR product was digested with *Nde*I and *Bam*HI and cloned into pSBET at these sites.

The same recombinant PCR protocol was used to introduce FHC mutations into His$_6$-hcTnT$_{70-170}$. To facilitate the selection of mutant clones, oligonucleotide primers were designed to contain a silent restriction site (see Table 1). The correct cDNA sequences were confirmed by automated sequencing at the University of Medicine and Dentistry of New Jersey DNA Core Facility, Robert Wood Johnson Medical School, Piscataway, NJ.

Expression and purification of hcTnT peptides

His$_6$-hcTnT$_{70-170}$ was expressed in *E. coli* BL21(DE3) pLysS (Studier et al., 1990). One-liter cultures in LB medium at OD_{590} = 0.6 were induced with 0.4 mM isopropyl-β-D-thiogalactopyranoside and grown for 4 h. The cells were collected by centrifugation and were lysed by adding 2 vol (v/w) of 9 M urea, 750 mM NaCl, 30 mM imidazole, 7.5 mM 2-mercaptoethanol, 15% glycerol, 30 mM Tris, pH 8.0. The lysate was sonicated and the cellular debris was removed by centrifugation at 22,000 rpm, 4°C, for 20 min in a Sorvall RC26Plus centrifuge equipped with a SLA-300 rotor. His$_6$-hcTnT$_{70-170}$ was separated from bacterial proteins in the supernatant by affinity chromatography on Ni-NTA agarose (Qiagen, Valencia, CA) equilibrated with 6 M urea, 500 mM NaCl, 20 mM imidazole, 5 mM 2-mercaptoethanol, 10% glycerol, 20 mM Tris, pH 8.0. Bound His$_6$-hcTnT$_{70-170}$ was eluted with 6 M urea, 100 mM NaCl, 100 mM imidazole, 5 mM 2-mercaptoethanol, 10% glycerol, 20 mM Tris, pH 8.0. Following dialysis into 1 mM dithiothreitol (DTT), 1 mM NaN_3, 0.5 mM EDTA, 50 mM Tris, pH 8.0, the His-tag was cleaved for 24 h at 30°C using 10 U of His$_6$-TEV protease per mg of peptide, leaving the C-terminal Gly of the tag as the N-terminal residue of the hcTnT fragment (Gly-hcTnT$_{70-170}$). Fol-

TABLE 1 Oligonucleotide primers used to prepare Gly-hcTnT$_{70-170}$ and to introduce FHC mutations

Primer	Primer sequence	Mutation	Coding primer sequence*	Restriction site
A	5′-CATATGTCGTACTACCATCACCATCACC-ATCACGATTACGATATCCCAACGACCGAA-AACCTGTATTTTCAGGGCATGTCTGACATA-GAAGAGGTGGTGG-3′	I79N	5′-CCCAACTTGGT*A*CCTCCCAAGA<u>A</u>CCCCGATGGAGAG-3′	*Kpn*I
B	5′-P-TATATCTCCTTCTTAAAGTTAAACAAA-ATTATTTC-3′	R92Q	5′-GACTTTGATGA*T*ATCCACC<u>A</u>GAAGCGCATGGAG-3′	*EcoRV*
C	5′-TAATAGGATCCATGCATTTTGGGGGTTA-CATCCAG-3′	R92W	5′-GACTTTGATGA*T*ATCCAC<u>T</u>GGAAGCGCATGGAG-3′	*Eco*RV
D	5′-P-ATCCTCAGCCTTCCTCCTGTTCTCC-3′	R92L	5′-GACTTTGATGA*T*ATCCAC<u>T</u>GGAAGCGCATGGAG-3′	*Eco*RV
E	5′-CCAACGACCGAAAACCTGTATTTTCAGGGC-TTCATGCCCAACTTGGTGCCTCCCAAGATC-3′	R92L	5′-GACTTTGATGA*T*ATCCACC<u>T</u>GAAGCGCATGGAG-3′	*Hind*III
F	5′-GCTAGTTATTGCTCAGCGGTGGCAG-3′	A104V	5′-CATCCACCGGAAGC<u>T</u>*T*ATGGAGAAGGACCTG-3′	*Pst*I
G	5′-CGATCCCGCGAAATTAATACGACTCAC-3′	F110I	5′-GACCTGAATGAGC*T*GCAGGCGCTGATCGAGGCTCAC-<u>A</u>TTGAGAACAGG-3′	*Pst*I
H	5′-GATCTTGGGAGGCACCAAGTTGGGCATGAA-GCCCTGAAAATACAGGTTTTCGGTCGTTGG-3′	ΔE160	5′-GCTGAAGAGAG*A*GCTCGACGA_GAGGAGGAGAACA-GGAGGAAG-3′	*Sac*I
		E163K	5′-GCTGAAGAGAG*A*GCTCGACGAGAGGAGGAG<u>A</u>AGAA-CAGGAGG-3′	*Sac*I

*Only the coding primer is shown in this table. These primers were used together with primer F in one primary PCR reaction. The reverse complements of these primers were used together with primer G in the second primary PCR. FHC mutations are underlined, mutations that introduce a silent restriction site are in italics.

lowing dialysis into 50 mM NaCl, 10 mM imidazole, pH 7.0, the His-tag and protease were removed on a Ni-NTA agarose column. The yield was ~20 mg/L of culture. The purity of the product was verified by SDS gel electrophoresis and reverse-phase high-performance liquid chromatography (HPLC). The mass was confirmed using electrospray mass spectroscopy with a peak at 12576.0 Da (expected mass: 12574.9 Da).

Tropomyosin binding

Chicken $\alpha\alpha$-TM was ligated to cyanogen-bromide-activated Sepharose (Sigma-Aldrich, St. Louis, MO) according to the manufacturer's protocol. TnT peptides were bound to TM-Sepharose and eluted with a gradient from 50–750 mM NaCl in 1 mM EGTA, 1 mM NaN_3, 10 mM imidazole, pH 6.5, at a flow rate of 0.5 ml/min. The protein concentration of each fraction was determined by the Bradford method (Pande and Murthy, 1994) and by densitometry of SDS-polyacrylamide gels using a Molecular Dynamics 300A computing densitometer (Molecular Dynamics, Sunnyvale, CA). The NaCl concentration in each fraction was determined by measuring the conductivity using a Radiometer Copenhagen model CDM3 conductivity meter and comparing it with the conductivity of NaCl standards.

Tropomyosin binding to F-actin

The effect of the Gly-hcTnT$_{70-170}$ fragments on the affinity of TM for actin was measured by co-sedimentation. Chicken pectoral muscle $\alpha\alpha$-TM was combined with the TnT peptides in a 1:1.2 molar ratio in 300 mM NaCl, 4 mM $MgCl_2$, 0.5 mM DTT, 10 mM 4-morpholineethanesulfonic acid (MES), pH 6.0, and centrifuged at 60,000 rpm, 20°C, for 25 min in a Beckman TLA-100 rotor to remove insoluble material. F-actin (5 μM final concentration) was combined with TM-TnT (0–6 μM final concentration) in the same buffer and centrifuged as before. The actin and TM were quantitated in SDS-polyacrylamide gels of the pellets using a Molecular Dynamics densitometer. The data were fit to the Hill equation to determine the affinity of TM for actin (SigmaPlot 5.0, Jandel Scientific, San Rafael, CA):

$$\nu = n[TM]^H/((1/K_{app})^H + [TM]^H), \quad (1)$$

where [TM] is the total concentration of tropomyosin in the sample, ν is the observed TM/actin density ratio at [TM], n is the maximal TM/actin density ratio, K_{app} is the apparent association constant of TM for actin, and H is the Hill coefficient.

Tropomyosin peptides

Synthetic N-terminal and C-terminal peptides of tropomyosin were commercially synthesized, purified to >95% purity by reverse-phase HPLC and analyzed by mass spectroscopy (SynPep, Dublin, CA). The N-terminal peptide, AcTM1aZip, consisted of the first 14 residues of rat α-TM and the last 18 residues of the GCN4 leucine zipper and was N-acetylated (Greenfield et al., 1998). The peptide is a dimer in solution, and given concentrations are dimer concentrations. The C-terminal peptide, TM9a36ox, consisted of the last 35 residues of rat α-TM (SWISS-PROT database accession number P04692) and an N-terminal cysteine. The N-terminal cysteines were air-oxidized to form a coiled-coil dimer of the peptide. Cross-linked peptide was separated from monomer by reverse phase HPLC.

Circular dichroism studies

Circular dichroism (CD) data were collected on an Aviv model 62D spectropolarimeter (Aviv, Lakewood, NJ) equipped with a five-sample thermal equilibration chamber as previously described (Greenfield and Hitchcock-DeGregori, 1995). TnT peptides were measured either alone or in mixtures with N- and C-terminal TM model peptides. The stoichiometry of Gly-hcTnT$_{70-170}$ binding to the AcTM1aZip-TM9a36ox complex (the overlap model) was determined by titrating an equimolar mixture of AcTM1aZip and TM9a36ox with the TnT-peptide and monitoring the effect on helical content at 222 nm.

Data were collected at a concentration of 17.5 μM for each peptide in 10 mM potassium phosphate, pH 6.5, and 10 μM for each peptide in 150 mM KCl, 10 mM potassium phosphate, pH 6.5, respectively. CD spectra were measured at 0°C, and the α-helical content of the TnT peptides was

calculated from ellipticity data using the neural network program, CDNN (Böhm et al., 1992). Thermal stability measurements were performed by following the ellipticity at 222 nm as a function of temperature between 0°C and 70°C. The midpoints of the thermal transitions (T_m) were determined from the first derivative of the melting curves.

General methods

Thin filament proteins were purified from chicken pectoral muscle using previously published methods. Skeletal actin was prepared from acetone powder (Hitchcock-DeGregori et al., 1982). $\alpha\alpha$-Tropomyosin was purified from the isoelectric precipitate from a troponin preparation (Hitchcock-DeGregori et al., 1985). SDS-polyacrylamide gel electrophoresis was performed as described by Laemmli (1970). Unless mentioned otherwise, the concentration of proteins and peptides was determined with the microbiuret method (Goa, 1953).

RESULTS

Design and purification of Gly-hcTnT$_{70-170}$

We have developed a model system to test the effects of FHC-causing mutations in TnT on interactions with TM and actin, the two major targets of TnT. Because most of the mutations are localized within a 100-residue region of TnT (Fig. 1), we defined a fragment of TnT spanning this region that retains the desired biological functions and is suitable for structural studies. Reasons for taking this approach are that TnT fragments are soluble, whereas full-length TnT is poorly soluble, and our disenchanting experience where similar studies using full-length TnT mutants gave conflicting results (Mukherjea et al., 1999; Tobacman et al., 1999; Redwood et al., 2000).

Previous studies of TnT fragments have been instrumental in specifying the functional domains of TnT. The design of the fragment for use in the present investigation was guided by the early work. Smillie and his co-workers showed that skeletal TnT$_{71-151}$, which corresponds to residues 101–181 in hcTnT, was 80% α-helical and bound to the N- and C-termini of TM (Pearlstone and Smillie, 1977; Pato et al., 1981). This fragment includes the region that is important for TnT to promote binding of TM to actin (Hill et al., 1992; Hinkle et al., 1999).

We elected to use a fragment spanning residues 70–170 of hcTnT that includes most of the region originally shown to bind well to TM (Jackson et al., 1975; Pearlstone and Smillie, 1977), extended toward the N-terminus to include eight of the nine sites of the FHC mutations in this region of TnT (see Fig. 1; the S179F mutation had not been reported at the time we designed the fragment (Ho et al., 2000)). The hcTnT cDNA was modified to express hcTnT$_{70-170}$ in *E. coli*, in a form that leaves an N-terminal Gly following enzymatic removal of a His$_6$-tag used for affinity purification (called Gly-hcTnT$_{70-170}$; see Materials and Methods, the Gly replaces a Ser at residue 69 in hcTnT). Functional analysis of Gly-hcTnT$_{70-170}$ showed that the fragment has the desired properties: it is soluble, α-helical, binds to TM, stabilizes the head-to-tail overlap region of TM, and promotes TM binding to actin. Its properties are similar to those of a longer fragment we expressed, hcTnT$_{58-181}$. We designed the shorter peptide for its potential advantage in structural studies and individually introduced the nine best-documented FHC-causing mutations into the Gly-hcTnT$_{70-170}$ construct (see Materials and Methods).

TABLE 2 TnT binding to TM and promotion of TM binding to actin

Mutation	Elution from TM column* ([NaCl] in mM)	K_{app} of TM for actin† (10^5 M^{-1})
No TnT	–	2.0±0.1
wt	260±16	6.6±0.4
I79N	283	6.7
R92L	146	5.2
R92Q	245	5.6
R92W	126	4.6
R94L	161	5.5
A104V	273	5.3
F110I	139	3.8
ΔE160	275	6.4
E163K	273	5.9

*Determined at 1 mM EGTA, 1 mM NaN_3, 10 mM imidazole, pH 6.5. Values are the average of two to three measurements. Wild type was measured seven times, and a standard deviation is given. Reproducibility of mutants was within 30 mM.

†Data collected at 300 mM NaCl, 4 mM $MgCl_2$, 0.5 mM DTT, 10 mM MES, pH 6.0, 20°C, were fit to the Hill equation. Standard errors of curve fitting to pooled data are $\pm 0.1 \times 10^5$ M^{-1}. Measurements were repeated 2–3 times except for no TnT and wt (6–10 times) shown with standard deviations.

Tropomyosin binding

Binding of the Gly-hcTnT$_{70-170}$ fragments to TM-Sepharose was measured by affinity chromatography, using the ionic strength for elution as an estimate of relative affinity for α-tropomyosin (Table 2). Fig. 2 shows typical elution profiles of R92W-Gly-hcTnT$_{70-170}$ and the wild-type fragment. Mutations that reduced TM affinity, in that they eluted at about half the ionic strength of wild type, were clustered between residues 92 and 110. Within this region, only R92Q and A104V, both relatively conservative changes, had no effect on TM binding. Mutations outside this region (I79N, E160, and E163K) were neutral.

Promotion of tropomyosin binding to actin by Gly-hcTnT$_{70-170}$

Wild-type Gly-hcTnT$_{70-170}$ promoted the binding of TM to actin, increasing the affinity approximately threefold, measured by co-sedimentation (Fig. 3 *A*, Table 2). All six mutations between residues 92 and 110 decreased the ability of Gly-hcTnT$_{70-170}$ to promote TM binding to actin (F110I and A104V are shown in Fig. 3, *B* and *C*, respectively;

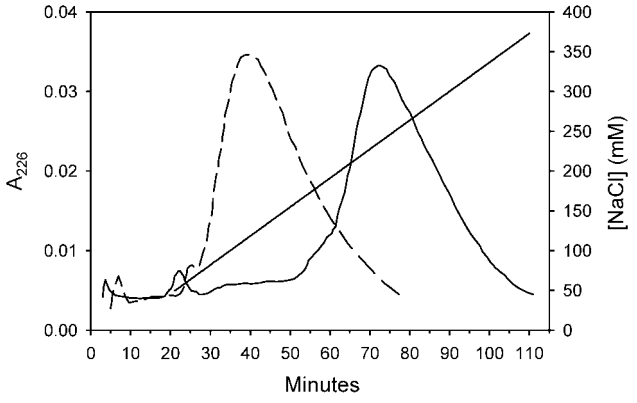

FIGURE 2 Binding of Gly-hcTnT$_{70-170}$ to tropomyosin-Sepharose. Typical elution profiles of wild-type (——) and R92W-Gly-hcTnT$_{70-170}$ (— — —). The straight line represents the NaCl concentration of the gradient. Conditions: 50–750 mM NaCl, 1 mM EGTA, 1 mM NaN_3, 10 mM imidazole, pH 6.5

Table 2). In contrast, mutations outside this region had little effect. The ability of TnT to increase the affinity of TM for actin seems to depend primarily on binding to TM. The A104V mutation that showed normal TM-binding, however, may directly affect TM-actin interaction.

Secondary structure and conformational stability

Circular dichroism was used to determine the secondary structure and thermal stability of wild-type and mutant Gly-hcTnT$_{70-170}$. The thermal denaturation of the TnT fragment and both TM peptides was fully reversible. None of the mutations affected the α-helical content of Gly-hcTnT$_{70-170}$ (90 $\pm$ 5% at 0°C, Table 3), but the thermal stability of the α-helix was altered by several mutations. The thermal stability of Gly-hcTnT$_{70-170}$ was concentration dependent, suggesting that the fragment forms homodimers or higher-order assemblies in solution. Therefore, all data were collected at the same concentration. Fig. 4 *A* shows the temperature dependence of the ellipticity at 222 nm, a measure of α-helix, of wt-Gly-hcTnT$_{70-170}$ and two mutants, A104V and F110I. The T_m values of the transitions are shown in Table 3. The thermal transitions of the mutants R92L, R92W, R94L, and F110I could not be fit to a single transition model. Although there was a minor transition with the T_m of the wild-type peptide, the major transition occurred with a much higher T_m, suggesting that these mutations stabilize the α-helix and/or the formation of homodimers. The most stable mutants are those that bind to tropomyosin with reduced affinity and are impaired in promoting TM binding to actin. A104V unfolded with a lower T_m than wild type; it binds to TM with normal affinity (Table 2). The effect of the other mutations on α-helical stability was minimal.

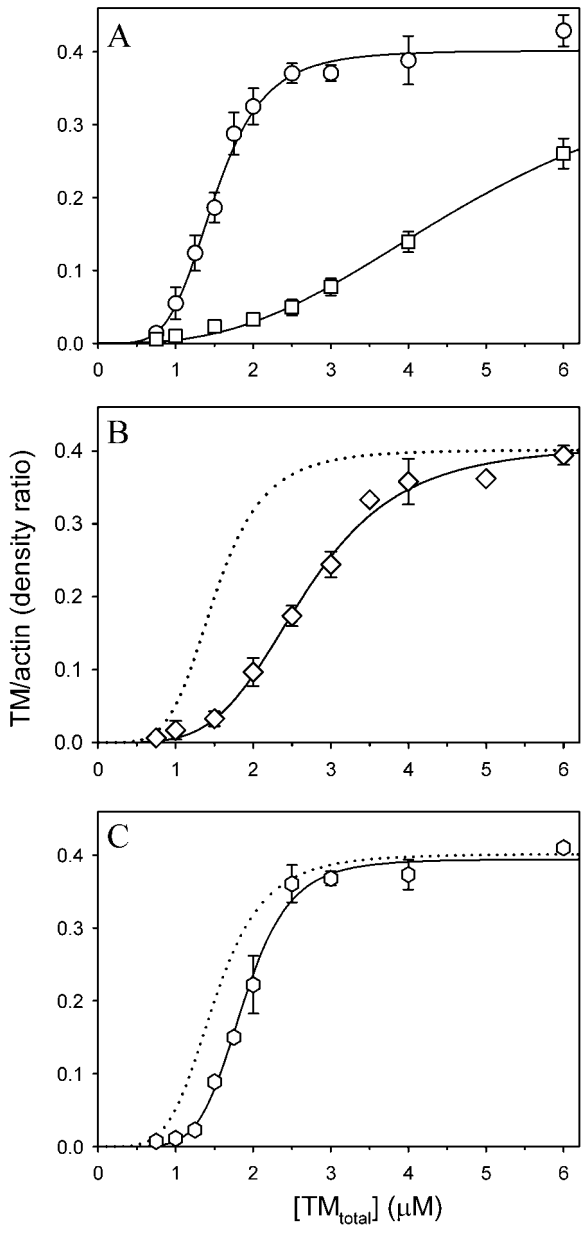

FIGURE 3 Tropomyosin binding to actin filaments. TM binding is the TM:actin ratio observed in densitometric analysis of Coomassie-Blue-stained SDS gels of the actin-containing pellets following centrifugation. The ratio observed at saturation reflects stoichiometric TM binding (TM:actin 1:7). (*A*) In the presence (○) and absence (□) of wt-Gly-hcTnT$_{70-170}$; (*B*) In the presence of F110I; (*C*) In the presence of A104V. The dotted line in *B* and *C* represents TM binding to actin in the presence of wt-Gly-hcTnT$_{70-170}$ taken from *A*. Error bars reflect the standard deviation of 3–10 independent measurements. Conditions: 300 mM NaCl, 4 mM $MgCl_2$, 0.5 mM DTT, 10 mM MES, pH 6.0, 20°C.

Stabilization of the N- to C-terminal tropomyosin overlap complex by Gly-hcTnT$_{70-170}$

Tropomyosin molecules associate head-to-tail along the actin filament and are proposed to overlap at their ends by about eight to nine amino acids (McLachlan and Stewart,

TABLE 3 Properties of wild-type and FHC mutant Gly-hcTnT$_{70\text{-}170}$ peptides and their complexes with AcTM1aZip and TM9a36ox

Peptide	% α-Helical content*	T_m peptide† (°C)	T_m ternary complex† (°C)	Increase in stability‡ (°C)
wt-Gly-hcTnT$_{70\text{-}170}$	90	33.5	36.1	7.6
I79N-Gly-hcTnT$_{70\text{-}170}$	90	32.9	35.9	7.6
R92L-Gly-hcTnT$_{70\text{-}170}$	93	32.8,44.4	35.1	4.1
R92Q-Gly-hcTnT$_{70\text{-}170}$	87	36.0	34.8	4.8
R92W-Gly-hcTnT$_{70\text{-}170}$	94	33.4,47.9	36.0	0.3
R94L-Gly-hcTnT$_{70\text{-}170}$	91	31.8,44.2	35.6	3.0
A104V-Gly-hcTnT$_{70\text{-}170}$	90	27.6	34.6	9.6
F110I-Gly-hcTnT$_{70\text{-}170}$	90	32.6,50.9	34.5	2.3
ΔE160-Gly-hcTnT$_{70\text{-}170}$	93	34.1	36.6	7.0
E163K-Gly-hcTnT$_{70\text{-}170}$	93	35.8	37.2	8.0
AcTM1aZip	85	22.7		
TM9a36ox	57	17.0		
AcTM1aZip + TM9a36ox			24.9§	5.4§
wt-Gly-hcTnT$_{70\text{-}170}$ + AcTM1aZip			29.4§	0.9§
wt-Gly-hcTnT$_{70\text{-}170}$ + TM9a36ox			31.3§	1.6§

Data were collected at a peptide concentration of 17.5 μM in 10 mM potassium phosphate, pH 6.5.
*Determined with neural network software CDNN (Böhm et al., 1992); accuracy of method, ±5%.
†Determined from the first derivative of the melting curve. Experiments with wt-Gly-hcTnT$_{70\text{-}170}$ and the TM peptides were repeated at least three times and showed that the reproducibility of T_m was usually better than 1°C.
‡The increase in stability is the difference between the T_m of the ternary complex and the T_m of the sum of Gly-hcTnT$_{70\text{-}170}$ and the binary complex of AcTM1aZip and TM9a36ox melting curves.
§Binary complex.

1975). Troponin promotes head-to-tail interaction, as measured using viscosity (Jackson et al., 1975) and increases the length of the cooperative unit of TM along the actin filament (Geeves and Lehrer, 1994).

To measure the influence of FHC mutations on the interaction of Gly-hcTnT$_{70-170}$ with the TM head-to-tail overlap region, we developed a model system employing two synthetic TM peptides. The N-terminal peptide, AcTM1aZip, consists of the first 14 residues of rat striated muscle α-TM (encoded by exon 1a) and the last 18 residues of the GCN4 leucine zipper. We previously solved the structure of AcTM1aZip using two-dimensional NMR (Greenfield et al., 1998). The C-terminal peptide, TM9a36ox, consists of the last 35 residues of rat striated muscle α-TM (encoded by exon 9a) and was cross-linked through an N-terminal cysteine. The mixture of the two peptides showed an increased thermal stability (+5.4°C) when compared with the sum of the individual components, indicating the formation of a complex. Although Gly-hcTnT$_{70-170}$ bound weakly to the C-terminal TM9a36ox (+1.6°C), the binding was slightly stronger than to the N-terminal AcTM1aZip (+0.9°C). However, it formed a stable ternary complex with the TM overlap peptides, increasing the T_m by 7.6°C (Fig. 4 *B*). When the TM overlap complex was titrated with increasing concentrations of Gly-hcTnT$_{70-170}$, the increase in ellipticity saturated at a stoichiometry of one TnT to one overlap complex (mol/mol) showing that the monomeric form of Gly-hcTnT$_{70-170}$ binds to TM.

The specificity of the peptide model of the TM overlap was validated in a similar binding study using two other synthetic peptides: TM9a39 (C-terminal 39 residues, encoded by rat exon 9a, specific to striated muscle TMs; similar to TM9a36ox, but 39 residues long and not cross-linked at the N-terminus) and TM9d39 (the corresponding C-terminal 39 residues encoded by rat exon 9d, expressed in smooth muscle and many nonmuscle TMs). Whereas TM9a39 formed a stable complex with AcTM1aZip and Gly-hcTnT$_{70-170}$, Gly-hcTnT$_{70-170}$ did not bind to TM9d39 or form a complex with TM9d39-AcTM1aZip (data not shown). This observation is supported by earlier work showing that the sequence encoded by exon 9a is required for TM to bind to TnT (Pearlstone and Smillie, 1982; Hammell and Hitchcock-DeGregori, 1996).

Most FHC mutations between residues 92 and 110 impaired the ability of Gly-hcTnT$_{70-170}$ to stabilize the TM head-to-tail overlap complex. The R92W and F110I mutations were most detrimental (see Fig. 4 *C* and Table 3). The stabilization by R92L, R92Q, and R94L was lower than that of the wild type whereas I79N, ΔE160, and E163K were unaffected. The stabilization of the overlap complex by A104V-Gly-hcTnT$_{70\text{-}170}$ was slightly greater than with wild type. This is probably due to a stabilizing effect of the TM overlap complex on the A104V fragment, which by itself is less stable than the wild-type TnT fragment.

In the CD experiments, the ability of Gly-hcTnT$_{70-170}$ to stabilize the TM overlap complex correlates with the effect of the mutations on the T_m of the TnT fragment: the higher the T_m, the less stabilization of the complex (Fig. 5). We were concerned that this relationship might be trivial because the calculated increase in stability is based on the difference between the T_m values of the sum of component melting curves and the melting curve of the mixture. However, the binding to the TM affinity column and the K_{app} of TM for actin in the presence of Gly-hcTnT$_{70-170}$ show the

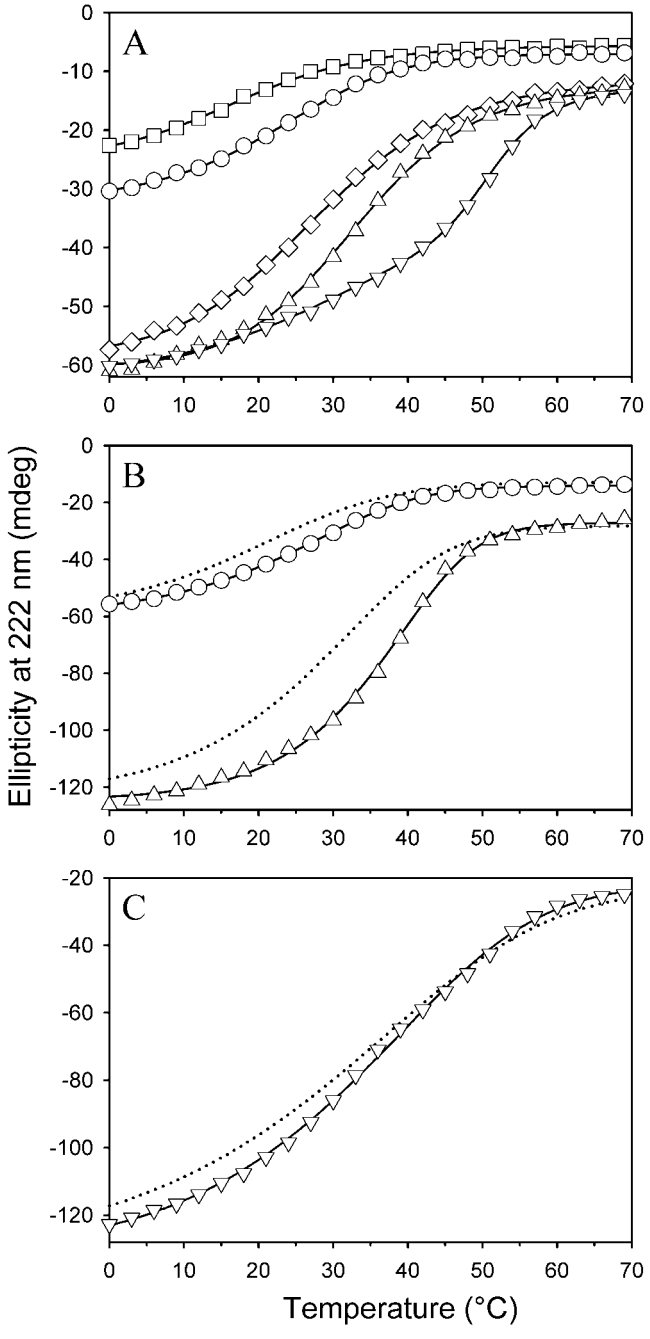

FIGURE 4 Effect of FHC-mutations on the temperature dependence of the unfolding of Gly-hcTnT$_{70-170}$, free (*A*) and in complex with TM peptides (*B* and *C*), determined by CD. Ellipticity was measured as a function of temperature in 10 mM potassium phosphate, pH 6.5, at a peptide concentration of 17.5 μM. (*A*) Thermal transitions of the TM peptides, AcTM1aZip (○), TM9a36ox (□), and the TnT fragments, wt-(△), F110I- (▽), and A104V-Gly-hcTnT$_{70-170}$ (◇); (*B*) Sum (· · ·) and equimolar mixture of the TM overlap complex, AcTM1aZip with TM9a36ox (○) and sum (· · ·) and equimolar mixture of the ternary complex of wt-Gly-hcTnT$_{70-170}$ with AcTM1aZip and TM9a36ox (△); (*C*) Sum (· · ·) and equimolar mixture of F110I-Gly-hcTnT$_{70-170}$ with AcTM1aZip and TM9a36ox (▽). The symbols in this figure represent every 15th data point.

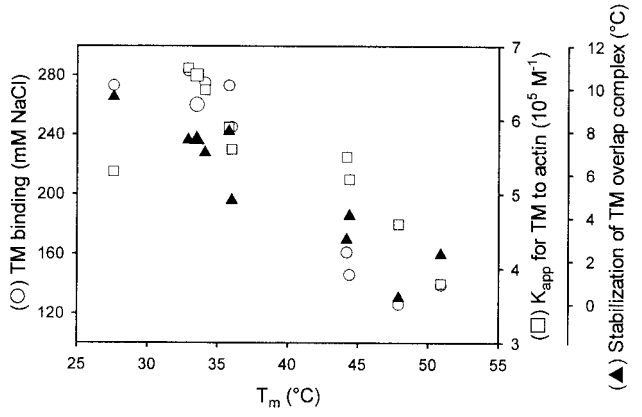

FIGURE 5 Correlation between the T_m of unfolding of Gly-hcTnT$_{70-170}$ and function of wt- and FHC-mutants. ○, TM binding as measured by the NaCl required for elution from TM-Sepharose (Table 2); □, the ability to promote TM binding to F-actin (Table 2); ▲, the stabilization of the Gly-hcTnT$_{70-170}$-TM overlap complex (Table 3). Symbols for wild-type (T_m = 33.5°C) are slightly larger.

same correlation with T_m (Fig. 5). The exception is the promotion of TM binding to actin by the mutant A104V, which we have suggested may directly influence actin binding.

All experiments in this study using TM9a36ox were done with a synthetic peptide designed using the sequence for rat α-TM in the SWISS-PROT database (accession number P04692). Recently, we realized that this sequence differs from that in the original references (Ruiz-Opazo et al., 1985; Ruiz-Opazo and Nadal-Ginard, 1987) and from our own sequence determination of rat striated α-TM DNA. Residue 279, an *f* position in the TM heptad repeats, is incorrectly listed as Lys in the SWISS-PROT database whereas it should be Asn. We repeated selected experiments with the correct N279-TM9a36ox. N279-TM9a36ox by itself is less stable than K279-TM9a36ox (−7.6°C), but the T_m values of binary complexes with AcTM1aZip or wt-Gly-hcTnT$_{70-170}$ and the ternary complex with AcTM1aZip and Gly-hcTnT$_{70-170}$ are within 1°C of those of K279-TM9a36ox. These results show that the Asn279Lys change does not affect binding of TM9a36ox to TnT and the N-terminus of TM.

DISCUSSION

Our studies show that FHC-causing mutations in hcTnT between residues 92 and 110 (R92L, R92Q, R92W, R94L, A104V, and F110I) impair TM-dependent functions of hcTnT and identify altered TM binding as a probable cause of disease. Mutations in TnT that affect the head-to-tail association of TM and the ability of TM to bind tightly to actin may be expected to negatively affect myofibrillar assembly, the cooperativity and extent of force development, and Ca^{2+}-dependence of contraction. Mutations out-

side this region (I79N, ΔE160, and E163K) had no effect on any parameter we studied and must cause disease by other mechanisms. The use of an hcTnT fragment and TM peptide models has allowed investigation of specific TnT-TM interactions and functions, giving new insights into the structural requirements for TnT activity.

The $hcTnT_{70–170}$ fragment used in our investigation is a highly conserved region of TnT, long known to bind to TM and to be highly α-helical (Pearlstone and Smillie, 1977; Perry, 1998). It is no surprise, therefore, that Gly-$hcTnT_{70–170}$ is highly helical. The amino acids introduced by the mutations are all well represented in α-helices or α-helical coiled-coils (Chou and Fasman, 1974; Cohen and Parry, 1990). Although the mutations do not reduce the helical content, some have dramatic effects on the stability in a way that correlates with TM binding. Mutations that increase the helical stability of Gly-$hcTnT_{70–170}$ (R92L, R92W, R94L, F110I, all with T_m values higher than physiological temperature) decrease its affinity for TM and for the TM peptide overlap model. The A104V mutation within the critical region reduces helical stability but has no effect on TM binding. The results suggest that one requirement for normal TM interaction is an α-helix of sufficient stability, but it cannot be too stable. An α-helix that is too stable may be too rigid to interact effectively with TM. Another possible explanation could be that Gly-$hcTnT_{70–170}$ self-associates. To bind stoichiometrically to TM, Gly-$hcTnT_{70–170}$ would have to be monomeric. Mutations that increase the stability of homodimers (or higher assemblies) may in turn decrease the ability of Gly-$hcTnT_{70–170}$ to interact with TM. The R92Q mutation has little effect on stability, but it does marginally reduce TM interaction, suggesting that additional parameters are important.

The ability of Gly-$hcTnT_{70–170}$ to promote binding of TM to actin filaments generally follows the same pattern as TM binding: mutations between residues 92 and 110 reduce affinity compared with wild type. We conclude from this that TnT must bind to TM to increase TM's affinity for actin. Gly-$hcTnT_{70–170}$ does not bind to actin alone in the conditions of our assays, suggesting that it has its effect by changing the ends of TM in a way that increases actin affinity. Not all mutations follow the pattern, inferring additional structural requirements. In particular, A104V is less effective than wild type in promoting TM binding to actin although the mutant binds normally to TM. Also, the E163K mutation, outside the critical residue 92–110 region, slightly impaired TM binding to actin.

The highly helical character of Gly-$hcTnT_{70–170}$ and earlier suggestions that α-helical regions of TnT bind to TM, possibly forming a triple helix (Nagano et al., 1980; Hitchcock et al., 1981; Ohtsuki and Nagano, 1982), led us to develop a model incorporating the Gly-$hcTnT_{70–170}$ fragment into the coiled-coil TM overlap complex. Examination of the $hcTnT_{70–170}$ sequence revealed a coiled-coil heptad repeat spanning residues 92–110, suggesting that this region may form a coiled-coil when it binds to TM. Possible β-turns at residues 80 and 122 (Chou and Fasman, 1979) flanking the coiled-coil region would allow TnT to bind to the C-terminus of TM in a parallel orientation (versus anti-parallel if there are no turns; see Fig. 1).

Fig. 6 shows a model of residues 92–110 of hcTnT binding to the TM overlap complex. The model was constructed starting from the four-helix bundle overlap complex proposed by McLachlan and Stewart (1975) that optimizes interchain interactions in the heptad repeat known to be important for coiled-coil stability: hydrophobic interactions between interface residues *a*-*d*, *a*-*a*, and *d*-*d*; ionic interactions, *e*-*g*; and packing of *a* against *g* and *d* against *e* at the interface. It is well accepted that striated muscle TMs overlap at the ends by eight to nine amino acids (Cohen et al., 1972; McLachlan and Stewart, 1975; Phillips et al., 1979), although the structure of the ends remains unresolved in crystals of TM (Whitby and Phillips, 2000).

The coiled-coil region of hcTnT (residues 92–110) was incorporated into the model by evaluating optimal interchain charge-charge and hydrophobic interactions between the C-terminal 25 amino acids of TM9a36 (encoded by striated muscle-specific exon 9a) and TnT because Gly-$hcTnT_{70–170}$ binds more strongly to the C-terminus of TM than to its N-terminus (see Results). In the model, the binding region of $hcTnT_{92–110}$ extends into the TM overlap region. Heptad positions *a* and *d* are symmetric in the model but positions *e* and *g* are not. Fig. 6 *A* shows the optimal alignments in both parallel and anti-parallel orientations of TnT. We favor the model of TnT oriented in parallel with TM (shown in Fig. 6 *B*) for the following reasons. There are more interactions favoring formation of a helix bundle: more than 15 in parallel versus 12 and 1 destabilizing interaction in the anti-parallel orientation (see legend to Fig. 6). The coiled-coil domain of TnT spans residues 263–281 of TM, the region of TM encoded by exon 9a that is required for TnT binding (Hammell and Hitchcock-DeGregori, 1996, 1997). Support for the parallel model also comes from NMR studies showing that the pK_a of His-79 in skeletal TnT (corresponding to His-109 in hcTnT) is increased when $skTnT_{71–151}$ binds to an N-terminal TM-peptide (Brisson et al., 1986). Although one would not normally expect a His in a *d* position of a coiled-coil, it could form a charge-charge interaction with Asp-280 in a *g* position in our model. Finally, the parallel model gives us the greatest insight into the effects of the FHC mutations that have the most severe effect on Gly-$hcTnT_{70–170}$ function. In the model, Arg-92 can form a hydrogen bond with Gln-263. The three R92 mutations would disrupt this interaction. The R92L and R92W, though stabilizing the helix, would alter the side-chain packing at the hydrophobic interface so as to weaken complex formation. In the parallel model, F110 extends into the overlap complex, potentially binding to hydrophobic residues at the extreme N-terminus, such as the acetylated Met-1 or Ile-4. The F110I mutation,

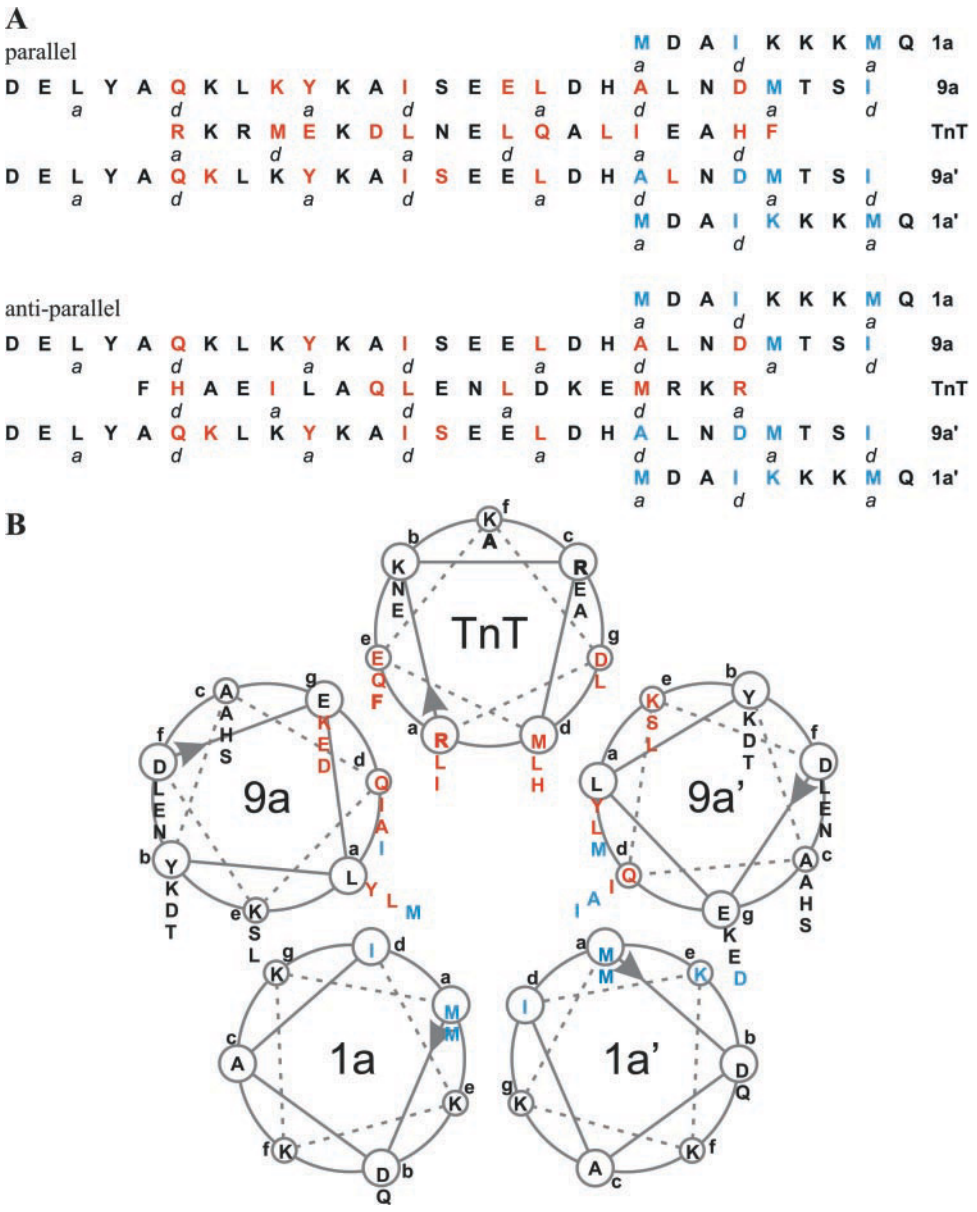

FIGURE 6 Coiled-coil model for the TnT-TM overlap complex. Possible parallel and anti-parallel coiled-coil interaction of $hcTnT_{92–110}$ with residues 1–9 of the N-terminus of TM and the C-terminus of TM (residues 258–284 encoded by exon 9a). Favorable interactions between the N-and C-termini of TM (marked in blue) cause TM to overlap by ~8–9 amino acids as proposed by McLachlan and Stewart (1975). The $hcTnT_{92–110}$ was docked to the sequence encoded by exon 9a to satisfy favorable interactions (marked in red). Positions within a heptad repeat are given in lowercase letters. To keep the figure simple, not all possible interactions are shown. (*A*) Linear open representation of the parallel (*top*) and anti-parallel (*bottom*) model; (*B*) Five-wheel helical representation of the parallel interaction. FHC mutation sites are marked bold.

the most severe mutation, would alter the packing. In both models, A104V is in an *f* position in the heptad repeat, explaining how it may influence actin binding of TM without impairing TM-TnT interaction.

Our results agree with previously published work on FHC-TnTs (full-length protein), where it is possible to compare the data. I79N-TnT and ΔE160-TnT have normal TM binding and promotion of binding of TM to actin (Lin et al., 1996; Tobacman et al., 1999; Homsher et al., 2000); F110I-TnT was impaired in its ability to promote TM binding to actin (Tobacman et al., 1999). A possible exception is the R92Q mutation, which in the full-length protein had no effect on TM binding to actin, whereas in the Gly-$hcTnT_{70–170}$ peptide it had small but probably real effects on function. Transgenic mice carrying the R92Q mutation showed myocyte disarray and dysfunctional hearts (Oberst et al., 1998).

Physiological studies measuring Ca^{2+} dependence of activity, force production, shortening velocity of the I79N, R92Q, and F110I mutations have been extensive. Systems

employed range from in vitro motility assays and actomyosin S1 ATPases (Lin et al., 1996; Tobacman et al., 1999; Homsher et al., 2000) to reconstituted myofibrils and myofibers (Morimoto et al., 1998; Yanaga et al., 1999; Harada et al., 2000; Szczesna et al., 2000) to adenovirus-transfected myocytes (Marian et al., 1997; Sweeney et al., 1998; Rust et al., 1999) and transgenic mice (Oberst et al., 1998; Tardiff et al., 1999; Lim et al., 2000; Knollmann et al., 2001; Miller et al., 2001). Unfortunately, the systems are complex and varied and have often produced conflicting results (reviewed in Hernandez et al., 2001). For this reason, we have not attempted to relate our findings to those of the FHC mutations in the physiological studies.

This research was supported by National Institutes of Health grant GM-36326 to S.E.H.-D. and N.J.G.

REFERENCES

Böhm, G., R. Muhr, and R. Jaenicke. 1992. Quantitative analysis of protein far UV circular dichroism spectra by neural networks. *Protein Eng.* 5:191–195.

Bonne, G., L. Carrier, P. Richard, B. Hainque, and K. Schwartz. 1998. Familial hypertrophic cardiomyopathy: from mutations to functional defects. *Circ. Res.* 83:580–593.

Brisson, J. R., K. Golosinska, L. B. Smillie, and B. D. Sykes. 1986. Interaction of tropomyosin and troponin T: a proton nuclear magnetic resonance study. *Biochemistry.* 25:4548–4555.

Cabral-Lilly, D., L. S. Tobacman, J. P. Mehegan, and C. Cohen. 1997. Molecular polarity in tropomyosin-troponin T co-crystals. *Biophys. J.* 73:1763–1770.

Chou, P. Y., and G. D. Fasman. 1974. Prediction of protein conformation. *Biochemistry.* 13:222–245.

Chou, P. Y., and G. D. Fasman. 1979. Prediction of beta-turns. *Biophys. J.* 26:367–373.

Cohen, C., D. L. Caspar, D. A. Parry, and R. M. Lucas. 1972. Tropomyosin crystal dynamics. *Cold Spring Harbor Symp. Quant. Biol.* 36:205–216.

Cohen, C., and D. A. Parry. 1990. Alpha-helical coiled coils and bundles: how to design an alpha-helical protein. *Proteins.* 7:1–15.

D'Cruz, L. G., C. Baboonian, H. E. Phillimore, R. Taylor, P. M. Elliott, A. Varnava, F. Davison, W. J. McKenna, and N. D. Carter. 2000. Cytosine methylation confers instability on the cardiac troponin T gene in hypertrophic cardiomyopathy. *J. Med. Genet.* 37:E18.

Flicker, P. F., G. N. Phillips, Jr., and C. Cohen. 1982. Troponin and its interactions with tropomyosin: an electron microscope study. *J. Mol. Biol.* 162:495–501.

Forissier, J. F., L. Carrier, H. Farza, G. Bonne, J. Bercovici, P. Richard, B. Hainque, P. J. Townsend, M. H. Yacoub, S. Faure, O. Dubourg, A. Millaire, A. A. Hagege, M. Desnos, M. Komajda, and K. Schwartz. 1996. Codon 102 of the cardiac troponin T gene is a putative hot spot for mutations in familial hypertrophic cardiomyopathy. *Circulation.* 94: 3069–3073.

Geeves, M. A., and S. S. Lehrer. 1994. Dynamics of the muscle thin filament regulatory switch: the size of the cooperative unit. *Biophys. J.* 67:273–282.

Goa, J. 1953. A micro biuret method for protein determination. *Scand. J. Clin. Lab. Invest.* 5:218–222.

Gordon, A. M., E. Homsher, and M. Regnier. 2000. Regulation of contraction in striated muscle. *Physiol. Rev.* 80:853–924.

Greenfield, N. J., and S. E. Hitchcock-DeGregori. 1995. The stability of tropomyosin, a two-stranded coiled-coil protein, is primarily a function of the hydrophobicity of residues at the helix- helix interface. *Biochemistry.* 34:16797–16805.

Greenfield, N. J., G. T. Montelione, R. S. Farid, and S. E. Hitchcock-DeGregori. 1998. The structure of the N-terminus of striated muscle alpha-tropomyosin in a chimeric peptide: nuclear magnetic resonance structure and circular dichroism studies. *Biochemistry.* 37:7834–7843.

Hammell, R. L., and S. E. Hitchcock-DeGregori. 1996. Mapping the functional domains within the carboxyl terminus of alpha-tropomyosin encoded by the alternatively spliced ninth exon. *J. Biol. Chem.* 271: 4236–4242.

Hammell, R. L., and S. E. Hitchcock-DeGregori. 1997. The sequence of the alternatively spliced sixth exon of alpha-tropomyosin is critical for cooperative actin binding but not for interaction with troponin. *J. Biol. Chem.* 272:22409–22416.

Harada, K., F. Takahashi-Yanaga, R. Minakami, S. Morimoto, and I. Ohtsuki. 2000. Functional consequences of the deletion mutation delta-Glu160 in human cardiac troponin T. *J. Biochem. (Tokyo).* 127:263–268.

Heeley, D. H., K. Golosinska, and L. B. Smillie. 1987. The effects of troponin T fragments T1 and T2 on the binding of nonpolymerizable tropomyosin to F-actin in the presence and absence of troponin I and troponin C. *J. Biol. Chem.* 262:9971–9978.

Hernandez, O. M., P. R. Housmans, and J. D. Potter. 2001. Pathophysiology of cardiac muscle contraction and relaxation as a result of alterations in thin filament regulation. *J. Appl. Physiol.* 90:1125–1136.

Higuchi, R. 1990. Recombinant PCR. *In* PCR Protocols: A Guide to Methods and Applications. M. A. Innis, D. H. Gelfand, J. J. Sninsky, and T. J. White, editors. Academic Press, San Diego. 177–183.

Hill, L. E., J. P. Mehegan, C. A. Butters, and L. S. Tobacman. 1992. Analysis of troponin-tropomyosin binding to actin. Troponin does not promote interactions between tropomyosin molecules. *J. Biol. Chem.* 267:16106–16113.

Hinkle, A., A. Goranson, C. A. Butters, and L. S. Tobacman. 1999. Roles for the troponin tail domain in thin filament assembly and regulation: a deletional study of cardiac troponin T. *J. Biol. Chem.* 274:7157–7164.

Hitchcock, S. E., C. J. Zimmerman, and C. Smalley. 1981. Study of the structure of troponin-T by measuring the relative reactivities of lysines with acetic anhydride. *J. Mol. Biol.* 147:125–151.

Hitchcock-DeGregori, S. E., S. F. Lewis, and T. M. Chou. 1985. Tropomyosin lysine reactivities and relationship to coiled-coil structure. *Biochemistry.* 24:3305–3314.

Hitchcock-DeGregori, S. E., S. Mandala, and G. A. Sachs. 1982. Changes in actin lysine reactivities during polymerization detected using a competitive labeling method. *J. Biol. Chem.* 257:12573–12580.

Ho, C. Y., H. M. Lever, R. DeSanctis, C. F. Farver, J. G. Seidman, and C. E. Seidman. 2000. Homozygous mutation in cardiac troponin T: implications for hypertrophic cardiomyopathy. *Circulation.* 102: 1950–1955.

Homsher, E., D. M. Lee, C. Morris, D. Pavlov, and L. S. Tobacman. 2000. Regulation of force and unloaded sliding speed in single thin filaments: effects of regulatory proteins and calcium. *J. Physiol.* 524:233–243.

Jackson, P., G. W. Amphlett, and S. V. Perry. 1975. The primary structure of troponin T and the interaction with tropomyosin. *Biochem. J.* 151: 85–97.

Knollmann, B. C., S. A. Blatt, K. Horton, F. de Freitas, T. Miller, M. Bell, P. R. Housmans, N. J. Weissman, M. Morad, and J. D. Potter. 2001. Inotropic stimulation induces cardiac dysfunction in transgenic mice expressing a troponin T (I79N) mutation linked to familial hypertrophic cardiomyopathy. *J. Biol. Chem.* 276:10039–10048.

Koga, Y., H. Toshima, A. Kimura, H. Harada, T. Koyanagi, H. Nishi, M. Nakata, and T. Imaizumi. 1996. Clinical manifestations of hypertrophic cardiomyopathy with mutations in the cardiac beta-myosin heavy chain gene or cardiac troponin T gene. *J. Cardiac Failure.* 2:S97–S103.

Laemmli, U. K. 1970. Cleavage of structural proteins during the assembly of the head of bacteriophage T4. *Nature.* 227:680–685.

Lim, D. S., L. Oberst, M. McCluggage, K. Youker, J. Lacy, F. DeMayo, M. L. Entman, R. Roberts, L. H. Michael, and A. J. Marian. 2000. Decreased left ventricular ejection fraction in transgenic mice expressing mutant cardiac troponin T-Q(92), responsible for human hypertrophic cardiomyopathy. *J. Mol. Cell. Cardiol.* 32:365–374.

Lin, D., A. Bobkova, E. Homsher, and L. S. Tobacman. 1996. Altered cardiac troponin T in vitro function in the presence of a mutation

implicated in familial hypertrophic cardiomyopathy. *J. Clin. Invest.* 97:2842–2848.

Marian, A. J., G. Zhao, Y. Seta, R. Roberts, and Q. T. Yu. 1997. Expression of a mutant (Arg92Gln) human cardiac troponin T, known to cause hypertrophic cardiomyopathy, impairs adult cardiac myocyte contractility. *Circ. Res.* 81:76–85.

McLachlan, A. D., and M. Stewart. 1975. Tropomyosin coiled-coil interactions: evidence for an unstaggered structure. *J. Mol. Biol.* 98: 293–304.

Miller, T., D. Szczesna, P. R. Housmans, J. Zhao, F. de Freitas, A. V. Gomes, L. Culbreath, J. McCue, Y. Wang, Y. Xu, W. G. Kerrick, and J. D. Potter. 2001. Abnormal contractile function in transgenic mice expressing an FHC-linked troponin T (179N) mutation. *J. Biol. Chem.* 276:3743–3755.

Moolman, J. C., V. A. Corfield, B. Posen, K. Ngumbela, C. Seidman, P. A. Brink, and H. Watkins. 1997. Sudden death due to troponin T mutations. *J. Am. Coll. Cardiol.* 29:549–555.

Morimoto, S., F. Yanaga, R. Minakami, and I. Ohtsuki. 1998. Ca^{2+}-sensitizing effects of the mutations at Ile-79 and Arg-92 of troponin T in hypertrophic cardiomyopathy. *Am. J. Physiol.* 275:C200–C207.

Mukherjea, P., L. Tong, J. G. Seidman, C. E. Seidman, and S. E. Hitchcock-DeGregori. 1999. Altered regulatory function of two familial hypertrophic cardiomyopathy troponin T mutants. *Biochemistry.* 38: 13296–13301.

Nagano, K., S. Miyamoto, M. Matsumura, and T. Ohtsuki. 1980. Possible formation of a triple-stranded coiled-coil region in tropomyosin-troponin T binding complex. *J. Mol. Biol.* 141:217–222.

Nakajima-Taniguchi, C., H. Matsui, Y. Fujio, S. Nagata, T. Kishimoto, and K. Yamauchi-Takihara. 1997. Novel missense mutation in cardiac troponin T gene found in Japanese patient with hypertrophic cardiomyopathy. *J. Mol. Cell. Cardiol.* 29:839–843.

Oberst, L., G. Zhao, J. T. Park, R. Brugada, L. H. Michael, M. L. Entman, R. Roberts, and A. J. Marian. 1998. Dominant-negative effect of a mutant cardiac troponin T on cardiac structure and function in transgenic mice. *J. Clin. Invest.* 102:1498–1505.

Ohtsuki, I., and K. Nagano. 1982. Molecular arrangement of troponin-tropomyosin in the thin filament. *Adv. Biophys.* 15:93–130.

Pan, B. S., A. M. Gordon, and J. D. Potter. 1991. Deletion of the first 45 NH_2-terminal residues of rabbit skeletal troponin T strengthens binding of troponin to immobilized tropomyosin. *J. Biol. Chem.* 266: 12432–12438.

Pande, S. V., and M. S. Murthy. 1994. A modified micro-Bradford procedure for elimination of interference from sodium dodecyl sulfate, other detergents, and lipids. *Anal. Biochem.* 220:424–426.

Pato, M. D., A. S. Mak, and L. B. Smillie. 1981. Fragments of rabbit striated muscle alpha-tropomyosin. II. Binding to troponin-T. *J. Biol. Chem.* 256:602–607.

Pearlstone, J. R., and L. B. Smillie. 1977. The binding site of skeletal alpha-tropomyosin on troponin-T. *Can. J. Biochem.* 55:1032–1038.

Pearlstone, J. R., and L. B. Smillie. 1982. Binding of troponin-T fragments to several types of tropomyosin: sensitivity to Ca^{2+} in the presence of troponin-C. *J. Biol. Chem.* 257:10587–10592.

Pearlstone, J. R., and L. B. Smillie. 1983. Effects of troponin-I plus-C on the binding of troponin-T and its fragments to alpha-tropomyosin: Ca^{2+} sensitivity and cooperativity. *J. Biol. Chem.* 258:2534–2542.

Perry, S. V. 1998. Troponin T: genetics, properties and function. *J. Muscle Res. Cell Motil.* 19:575–602.

Phillips, G. N., Jr., E. E. Lattman, P. Cummins, K. Y. Lee, and C. Cohen. 1979. Crystal structure and molecular interactions of tropomyosin. *Nature.* 278:413–417.

Redwood, C., K. Lohmann, W. Bing, G. M. Esposito, K. Elliott, H. Abdulrazzak, A. Knott, I. Purcell, S. Marston, and H. Watkins. 2000. Investigation of a truncated cardiac troponin T that causes familial hypertrophic cardiomyopathy: Ca(2+) regulatory properties of reconstituted thin filaments depend on the ratio of mutant to wild-type protein. *Circ. Res.* 86:1146–1152.

Ruiz-Opazo, N., and B. Nadal-Ginard. 1987. Alpha-tropomyosin gene organization. Alternative splicing of duplicated isotype-specific exons accounts for the production of smooth and striated muscle isoforms. *J. Biol. Chem.* 262:4755–4765.

Ruiz-Opazo, N., J. Weinberger, and B. Nadal-Ginard. 1985. Comparison of alpha-tropomyosin sequences from smooth and striated muscle. *Nature.* 315:67–70.

Rust, E. M., F. P. Albayya, and J. M. Metzger. 1999. Identification of a contractile deficit in adult cardiac myocytes expressing hypertrophic cardiomyopathy-associated mutant troponin T proteins. *J. Clin. Invest.* 103:1459–1467.

Schenk, P. M., S. Baumann, R. Mattes, and H. H. Steinbiss. 200. 1995. Improved high-level expression system for eukaryotic genes in *Escherichia coli* using T7 RNA polymerase and rare ArgtRNAs. *Biotechniques.* 19:196–198.

Studier, F. W., A. H. Rosenberg, J. J. Dunn, and J. W. Dubendorff. 1990. Use of T7 RNA polymerase to direct expression of cloned genes. *Methods Enzymol.* 185:60–89.

Sweeney, H. L., H. S. Feng, Z. Yang, and H. Watkins. 1998. Functional analyses of troponin T mutations that cause hypertrophic cardiomyopathy: insights into disease pathogenesis and troponin function. *Proc. Natl. Acad. Sci. U.S.A.* 95:14406–14410.

Szczesna, D., R. Zhang, J. Zhao, M. Jones, G. Guzman, and J. D. Potter. 2000. Altered regulation of cardiac muscle contraction by troponin T mutations that cause familial hypertrophic cardiomyopathy. *J. Biol. Chem.* 275:624–630.

Tardiff, J. C., T. E. Hewett, B. M. Palmer, C. Olsson, S. M. Factor, R. L. Moore, J. Robbins, and L. A. Leinwand. 1999. Cardiac troponin T mutations result in allele-specific phenotypes in a mouse model for hypertrophic cardiomyopathy. *J. Clin. Invest.* 104:469–481.

Thierfelder, L., H. Watkins, C. MacRae, R. Lamas, W. McKenna, H. P. Vosberg, J. G. Seidman, and C. E. Seidman. 1994. Alpha-tropomyosin and cardiac troponin T mutations cause familial hypertrophic cardiomyopathy: a disease of the sarcomere. *Cell.* 77:701–712.

Tobacman, L. S., D. Lin, C. Butters, C. Landis, N. Back, D. Pavlov, and E. Homsher. 1999. Functional consequences of troponin T mutations found in hypertrophic cardiomyopathy. *J. Biol. Chem.* 274:28363–28370.

Varnava, A., C. Baboonian, F. Davison, L. de Cruz, P. M. Elliott, M. J. Davies, and W. J. McKenna. 1999. A new mutation of the cardiac troponin T gene causing familial hypertrophic cardiomyopathy without left ventricular hypertrophy. *Heart.* 82:621–624.

Watkins, H., W. J. McKenna, L. Thierfelder, H. J. Suk, R. Anan, A. O'Donoghue, P. Spirito, A. Matsumori, C. S. Moravec, J. G. Seidman, and C. E. Seidman. 1995. Mutations in the genes for cardiac troponin T and alpha-tropomyosin in hypertrophic cardiomyopathy. *N. Engl. J. Med.* 332:1058–1064.

Whitby, F. G., and G. N. Phillips, Jr. 2000. Crystal structure of tropomyosin at 7 angstroms resolution. *Proteins.* 38:49–59.

White, S. P., C. Cohen, and G. N. Phillips, Jr. 1987. Structure of co-crystals of tropomyosin and troponin. *Nature.* 325:826–828.

Yanaga, F., S. Morimoto, and I. Ohtsuki. 1999. Ca^{2+} sensitization and potentiation of the maximum level of myofibrillar ATPase activity caused by mutations of troponin T found in familial hypertrophic cardiomyopathy. *J. Biol. Chem.* 274:8806–8812.